RESEARCH ARTICLE

Disease Models & Mechanisms 4, 400-410 (2011) doi:10.1242/dmm.006148

Human cardiomyopathy mutations induce myocyte hyperplasia and activate hypertrophic pathways during cardiogenesis in zebrafish

Jason R. Becker[1,2,*], Rahul C. Deo[1], Andreas A. Werdich[1,‡], Daniela Panàkovà[1,3], Shannon Coy[1] and Calum A. MacRae[1,3]

SUMMARY

To assess the effects during cardiac development of mutations that cause human cardiomyopathy, we modeled a sarcomeric gene mutation in the embryonic zebrafish. We designed morpholino antisense oligonucleotides targeting the exon 13 splice donor site in the zebrafish cardiac troponin T (*tnnt2*) gene, in order to precisely recapitulate a human TNNT2 mutation that causes hypertrophic cardiomyopathy (HCM). HCM is a disease characterized by myocardial hypertrophy, myocyte and myofibrillar disarray, as well as an increased risk of sudden death. Similar to humans with HCM, the morphant zebrafish embryos displayed sarcomere disarray and there was a robust induction of myocardial hypertrophic pathways. Microarray analysis uncovered a number of shared transcriptional responses between this zebrafish model and a well-characterized mouse model of HCM. However, in contrast to adult hearts, these embryonic hearts developed cardiomyocyte hyperplasia in response to this genetic perturbation. The re-creation of a human disease-causing TNNT2 splice variant demonstrates that sarcomeric mutations can alter cardiomyocyte biology at the earliest stages of heart development with distinct effects from those observed in adult hearts despite shared transcriptional responses.

INTRODUCTION

In the last two decades, genetic studies of inherited forms of human cardiomyopathy have offered important insights into the fundamental biology of myocardial hypertrophy and heart failure. Many of the causal genes for inherited hypertrophic cardiomyopathy (HCM) encode for proteins involved in the proper function of the cardiac sarcomere. However, substantial pleiotropy is seen for many cardiomyopathy genes. Even within families harboring the same mutation there is significant variation in the extent of hypertrophy, the risk of arrhythmias or the progression to heart failure (Alcalai et al., 2007; Arad et al., 2002). Furthermore, different mutations in a single gene can lead to either HCM or dilated cardiomyopathy (DCM) (Seidman and Seidman, 2001). The major modifiers regulating this phenotypic diversity have not been defined.

Evidence is emerging of significant overlap between the pathways regulating cell division and those driving cardiac hypertrophy (Ahuja et al., 2007). Nuclear division and polyploidy are observed in the later stages of human heart failure and resolve with ventricular unloading, but cellular dynamics earlier in hypertrophy have not yet been explored (Rivello et al., 2001). The limited capacity for cell division in adult mammalian cardiomyocytes leads to the chronic activation of cell division pathways; these same pathways are thought to drive the changes in cardiomyocyte differentiation seen in the hypertrophic process. The effects of manipulating cell division pathways on myocardial growth are diverse and might involve epigenetic mechanisms with complex inheritance patterns (Wagner et al., 2008).

In an effort to define the earliest elements of the response to hypertrophic stimuli, we have generated a zebrafish model of a human cardiac troponin T (TNNT2) mutation known to cause HCM. This model not only facilitates the study of the initial developmental effects of a primary cause of hypertrophic cardiomyopathy, but also allows the systematic study of genetic and environmental modifiers before the effects of chronic myocardial remodeling supervene.

In order to precisely recapitulate a human TNNT2 disease mutation in the zebrafish, we designed morpholino antisense oligonucleotides (oligos) that target the intron 13 splice donor site in the zebrafish cardiac troponin T (*tnnt2*) mRNA. The resultant sequence is orthologous to an established human TNNT2 splice mutant and its expression is importantly under the control of the native zebrafish *tnnt2* promoter. Morphant hearts exhibited disrupted sarcomere formation and showed induction of a pathological transcriptional response during the earliest stages of cardiogenesis. In addition, in these embryonic hearts, we confirmed that Tnnt2 mutations lead to significant myocardial hyperplasia. We also demonstrate that this Tnnt2 mutation perturbs normal cardiomyocyte Ca^{2+} handling, suggesting that the arrhythmic risk in the context of sarcomeric protein mutations does not simply reflect the consequences of cellular disarray and scarring. Lastly, once the genetic stimulus is eliminated, sarcomerogenesis normalizes. Taken together, these data highlight the distinctive initial responses of the embryonic heart to a primary hypertrophic

[1]Harvard Medical School, Division of Cardiology, Massachusetts General Hospital, Boston, MA 02129, USA
[2]Vanderbilt University Medical Center 2220 Pierce Avenue, 340 PRB Nashville, TN 37232-6300, USA
[3]Harvard Medical School, Division of Cardiology, Brigham and Women's Hospital, Boston, MA 02115, USA
*Author for correspondence (jason.r.becker@vanderbilt.edu)
‡Present address: Case Western Reserve University, Department of Physiology and Biophysics, 10900 Euclid Avenue, Cleveland, OH 44106, USA

Received 27 May 2010; Accepted 11 November 2010

stimulus, despite evidence of substantial sharing of sarcomeric biology and transcriptional pathways with adult myocardium.

RESULTS

The zebrafish Tnnt2 splice variant genocopies the human disease-causing TNNT2 splice variant

In order to precisely recapitulate an autosomal dominant hypertrophic cardiomyopathy mutation, we chose to model a mutation in the splice donor site of exon 15 in human *TNNT2* (Thierfelder et al., 1994). The mutant *TNNT2* mRNA splice products either exclude exon 15 or use a cryptic splice site that changes the reading frame and leads to a premature stop codon (Fig. 1A). We used a morpholino (TNNT2sp MO) to target the splice donor site in zebrafish *tnnt2* exon 13, which is the ortholog of human *TNNT2* exon 15 (detailed sequence data for zebrafish *tnnt2* in supplementary material Fig. S1). The resulting morphant splice product excludes zebrafish *tnnt2* exon 13 (Fig. 1B), causing a disruption in the C-terminus of the zebrafish Tnnt2 protein at the identical position to that mutated in humans (Fig. 1C). This morpholino allows the creation of a dominant mutation in Tnnt2 while retaining the full control of the native zebrafish *tnnt2* promoter. In an effort to model the nature of the human disease as precisely as possible, the TNNT2sp MO was dosed so that the wild-type *tnnt2* transcript was reduced by approximately 50% (Fig. 1B).

Morphant ventricles exhibit restrictive physiology and diminished contractility

There was no evidence of non-cardiac or off-target morpholino effects in the TNNT2sp morphants and the embryos developed at a normal rate (Fig. 2A). Gross morphological examination of the morphants showed a smaller ventricle, dilated atria and pericardial edema compared with controls (Fig. 2B). Measurement of the ventricular internal chamber dimensions at end diastole [end-diastolic diameter (EDD; largest ventricular diameter)] and end systole [end-systolic diameter (ESD; smallest ventricular diameter)] confirmed substantial reductions in EDD in morphants compared with control embryos (control EDD 55±1.1 μm; TNNT2sp MO EDD 31±1.6 μm; $P<0.005$, $n=5$). ESD was also significantly decreased but to a lesser extent (control ESD 25±1.4 μm; TNNT2sp MO ESD 21±0.68 μm; $P<0.04$, $n=5$) (Fig. 2C). TNNT2sp morphants also exhibited significant reductions in ventricular fractional shortening (FS) (control FS 0.54; TNNT2sp MO FS 0.33; $P<0.005$, $n=5$) (Fig. 2D). Videos of control and TNNT2sp morphant hearts are included in supplementary material Movies 1 (control) and 2 (TNNT2sp morphant) (both at 72 hpf).

Defective *tnnt2* splicing causes sarcomeric disarray in the embryonic heart

Mutant sarcomeric proteins frequently perturb sarcomere assembly. Therefore, we performed electron microscopy of control and TNNT2sp morphants to explore the ultrastructure of the embryonic heart. There was marked sarcomeric disarray in the TNNT2sp morphants, which was not present in control embryos at 96 hpf (Fig. 3A). The altered mRNA splicing induced by injection of the TNNT2sp MO is temporary and the morpholino effect is gradually diluted through cell division during development. We tested 8- and 21-day-old embryos that had recovered from the initial morpholino injection to determine whether disruption of early sarcomere structure persists despite the elimination of the primary genetic stimulus. Although, sarcomere disarray was apparent in 8-dpf embryos, by 21 dpf there were no ultrastructural differences observed between control- and TNNT2sp-MO-injected embryos (Fig. 3A).

Tnnt2 mutation induces embryonic myocardial hyperplasia

Sarcomeric mutations are a stimulus for cardiomyocyte hypertrophy, which, in adult mammalian cardiomyocytes, seems to occur in isolation with no evidence of cardiomyocyte division (Ahuja et al., 2007). The effects of typical hypertrophic stimuli on embryonic cardiomyocytes remain unclear. We quantified the total number of cardiomyocytes in control and TNNT2sp morphant embryos using a *cmlc2*::DsRed-nuc transgenic zebrafish reporter line [red fluorescent protein (DsRed-nuc) expressed under the control of the *cardiac myosin light chain-2* (*cmlc-2*) promoter] that fluorescently labels the nuclei of differentiated cardiomyocytes (Mably et al., 2003). These embryos were injected with TNNT2sp or control morpholino and cardiomyocyte nuclei were counted at 48 and 96 hpf. The nuclei numbers were similar at 48 hpf (control 197±22, $n=4$; TNNT2sp MO 204±14, $n=5$; P=NS) but, at 96 hpf, the TNNT2sp morphant hearts had approximately 26% more DsRed-positive nuclei than control hearts (control 247±7, $n=4$; TNNT2sp MO 311±14, $n=3$; $P<0.03$) (Fig. 3B). There was no evidence of bi-nucleated cardiomyocytes; therefore, total nuclear count correlates with total cardiomyocyte count. Ventricular cardiomyocyte cell size was measured to determine whether morphant cardiomyocytes underwent cellular hypertrophy secondary to the presence of mutant *tnnt2* splice product. Morphant ventricular cardiomyocytes did not undergo hypertrophy but were actually slightly smaller than control cardiomyocytes (control 109±6 μm^2, $n=15$; TNNT2sp MO 94±4 μm^2, $n=11$; $P<0.04$) (Fig. 3C).

Tnnt2 mutations perturb embryonic cardiomyocyte Ca^{2+} handling

Abnormal cardiomyocyte Ca^{2+} handling is thought to be a stimulus for arrhythmias in patients with sarcomeric gene mutations (Baudenbacher et al., 2008; Knollmann et al., 2003). We performed high-resolution Ca^{2+} imaging in order to determine the effects of sarcomeric mutation on cardiomyocyte Ca^{2+} handling during early heart development. The most striking difference between TNNT2sp morphant and control embryos was the shortening of the Ca^{2+} transient duration (CTD50) in the TNNT2sp morphants. This shortening was observed in both atrium and ventricle (Fig. 4C) (supplementary material Table S1). Zebrafish null for Tnnt2 (TNNT2atg) were also analyzed to determine whether the reduction in CTD50 was a distinctive feature of the mutant RNA resulting from the TNNT2sp MO or was a result of loss or absence of wild-type Tnnt2 protein. TNNT2atg hearts, which never contract, exhibited a significant reduction of CTD50 in the atrioventricular canal, but did not develop significant reductions of CTD50 in the atrium or ventricle. In contrast to changes seen in CTD50, diastolic Ca^{2+} levels and Ca^{2+} transient amplitudes in TNNT2sp morphants were not significantly different to control hearts across multiple locations (Fig. 4A,B; supplementary material Fig. S2 and Table S1). However, TNNT2atg hearts showed significant changes

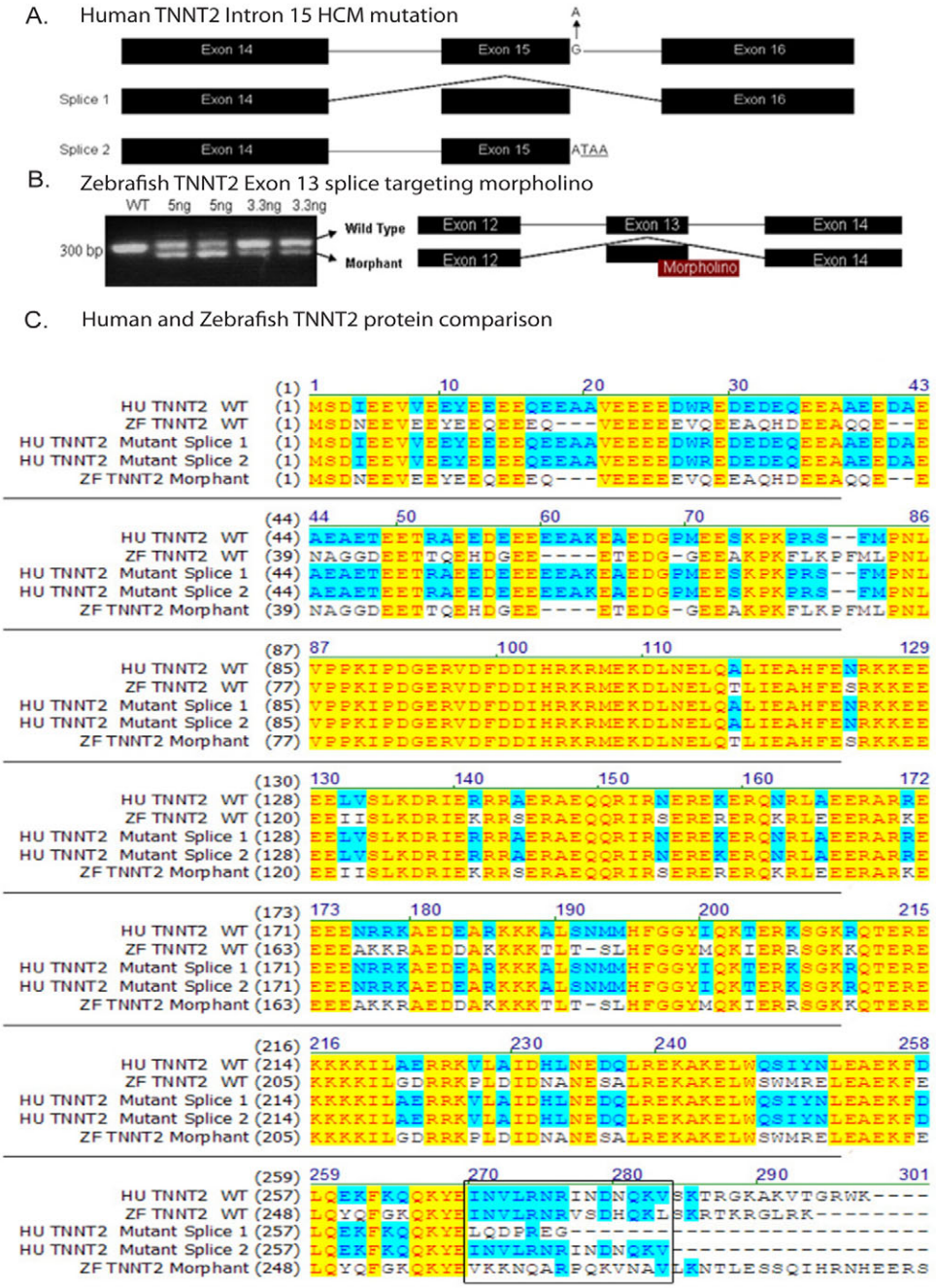

Fig. 1. A human TNNT2 splice mutation is copied in zebrafish by using a splice targeting morpholino. (A) A human *TNNT2* intron 15 mutation that causes two different mutant splice products of *TNNT2*. (B) Morpholino targeting of zebrafish *tnnt2* exon 13 causes mis-splicing of *tnnt2* mRNA, resulting in a smaller gene product (smaller band on agarose gel). (C) Comparison of human and zebrafish TNNT2 wild-type and mutant protein sequences (box around exon 15 human/exon 13 zebrafish).

compared with controls in these two parameters in multiple different locations (Fig. 4A,B; supplementary material Table S1). These data suggest that the splice mutant Tnnt2 protein results in an early 'gain-of-function' effect on embryonic cardiomyocyte Ca^{2+} handling, quite distinct from the effects of null *tnnt2* alleles (TNNT2atg).

Transcriptional responses to mutant Tnnt2

The typical gene expression signature induced in the setting of sarcomeric dysfunction in adult animals is referred to as reactivation of the 'fetal gene program'. This group of genes includes the cardiac natriuretic peptides NPPA and NPPB, as well as isoform switching of myosin heavy chain genes. We were interested to determine whether these transcriptional pathways could be pathologically induced during cardiac development. We performed a microarray analysis of gene expression in TNNT2sp- and control-MO-injected morphants. Interestingly, we saw a significant induction of the zebrafish ortholog of NPPA (average 2.9-fold increase; Q value<0.03). A direct comparison of myosin heavy chain isoform changes from zebrafish to mammals cannot be made because, to date, no zebrafish ortholog of *myh7* (beta-myosin heavy chain) has been identified. Two cardiac myosin heavy chain genes have been characterized in the zebrafish, *myh6* (also known as atrial myosin heavy chain) and *vmhc* (ventricular myosin heavy chain).

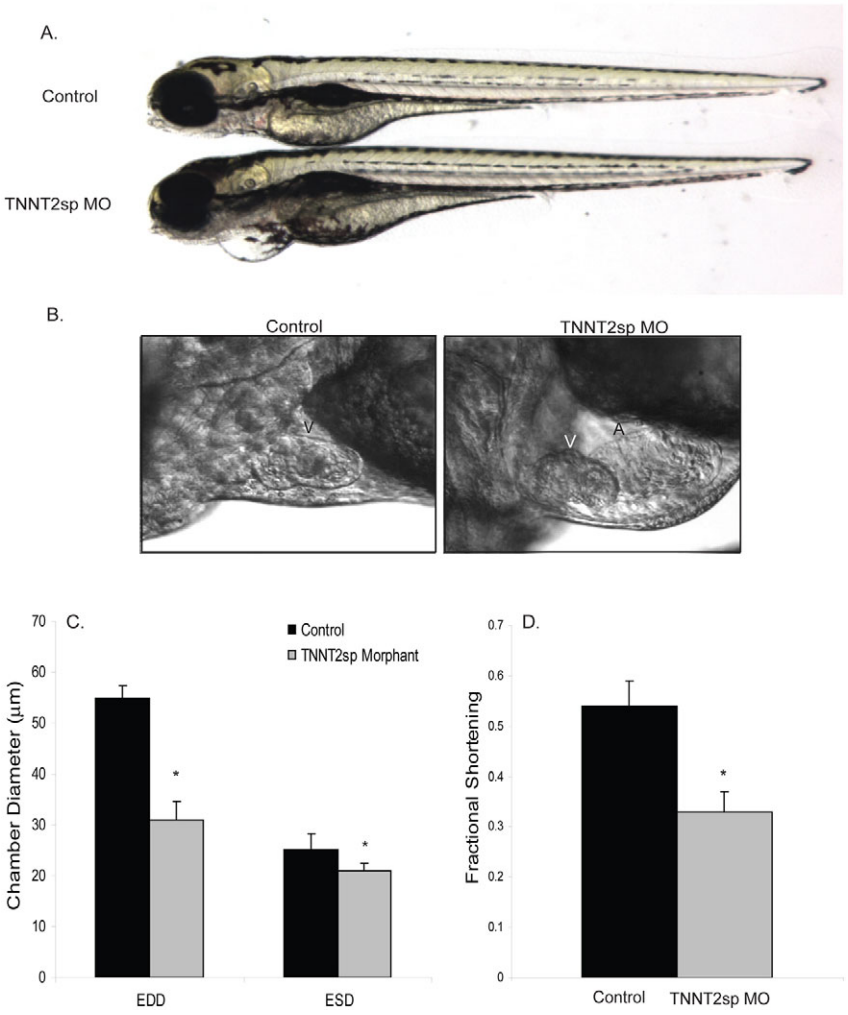

Fig. 2. TNNT2sp morphants have reduced ventricular dimensions and impaired ventricular function. (A) Comparison of control-injected (top) and TNNT2sp morphant (bottom) embryos at 96 hpf. (B) Representative high-magnification image of control (left) and TNNT2sp morphant (right) heart (A, atria; V, ventricle; atria not visible in control). (C) Chamber dimensions in control (black bar) and TNNT2sp morphants (gray bar). (D) FS in control (black bar) and TNNT2sp morphants (gray bar). **P*<0.05; *n*=5 for all measurements. All data expressed as mean + s.e.m.

Zebrafish Myh6 and Vmhc proteins are more closely related to mouse Myh6 (α-myosin heavy chain) than mouse Myh7 (NCBI, Blast Protein Alignment). Notably, zebrafish *myh6* gene expression was increased 1.73-fold in the TNNT2sp morphant embryos, whereas *vmhc* expression was not significantly changed (Fig. 5A, black bar; *Q* value=0.11). The other sarcomeric genes evaluated on the microarray are presented for comparison. Of note, one probe specifically bound to exon 13 of zebrafish *tnnt2*, allowing us to independently assess the efficacy of our TNNT2sp MO. The TNNT2sp morphants had a significant reduction in wild-type *tnnt2* mRNA compared with embryos injected with a control morpholino [Fig. 5A, white bar labeled 'tnnt2 (exon 13)'; *Q* value=0.006]. A second *tnnt2* probe that bound the 3′ untranslated region of *tnnt2* mRNA also showed reduced levels of expression in the TNNT2sp morphants [Fig. 5A, white bar labeled 'tnnt2 (3′ UTR)'; *Q* value=0.06].

Given the significant reduction in CTD50 seen in our TNNT2sp morphants, we evaluated the list of differentially expressed genes to identify potential transcriptional differences that might explain these effects. In the morphants, we found upregulation of several genes that are known to regulate cardiomyocyte Ca^{2+} homeostasis – the cardiac sodium/calcium exchanger (*slc8a1a*), calsequestrin 2 (*casq2*), sarcalumenin (*srl*) and calpastatin (*cast*) (Harris et al., 2006; Kubalova et al., 2004; Yoshida et al., 2005) (Fig. 5B).

We next undertook formal analysis of the microarray datasets for pathway enrichment in the morphant using FuncAssociate (Berriz et al., 2003). The only genetic pathway that was significantly perturbed in TNNT2sp morphants was a group of genes classified under the gene ontology term 'hormone activity' (GO:0005179), all of which were coordinately downregulated. The specific genes associated with this pathway included growth hormone releasing hormone (*ghrh*), parathyroid hormone (*pth1a*), proopiomelanocortin (*pomca*) and urotensin2a (*uts2a*) (Fig. 5C).

To confirm that the microarray accurately reflects gene expression changes, we performed quantitative reverse-transcriptase PCR (qPCR) on select upregulated (>twofold increased) and downregulated (>50% decreased) genes identified on the microarray. The microarray and qPCR results show similar levels of up- or down-regulation (Fig. 5D).

Lastly, to explore the extent to which the embryonic zebrafish TNNT2sp transcriptional responses parallel those in adult mammalian HCM models, we compared our whole-embryo dataset with an HCM gene expression dataset from mouse ventricular tissue generated with Polony Multiplex Analysis of Gene Expression

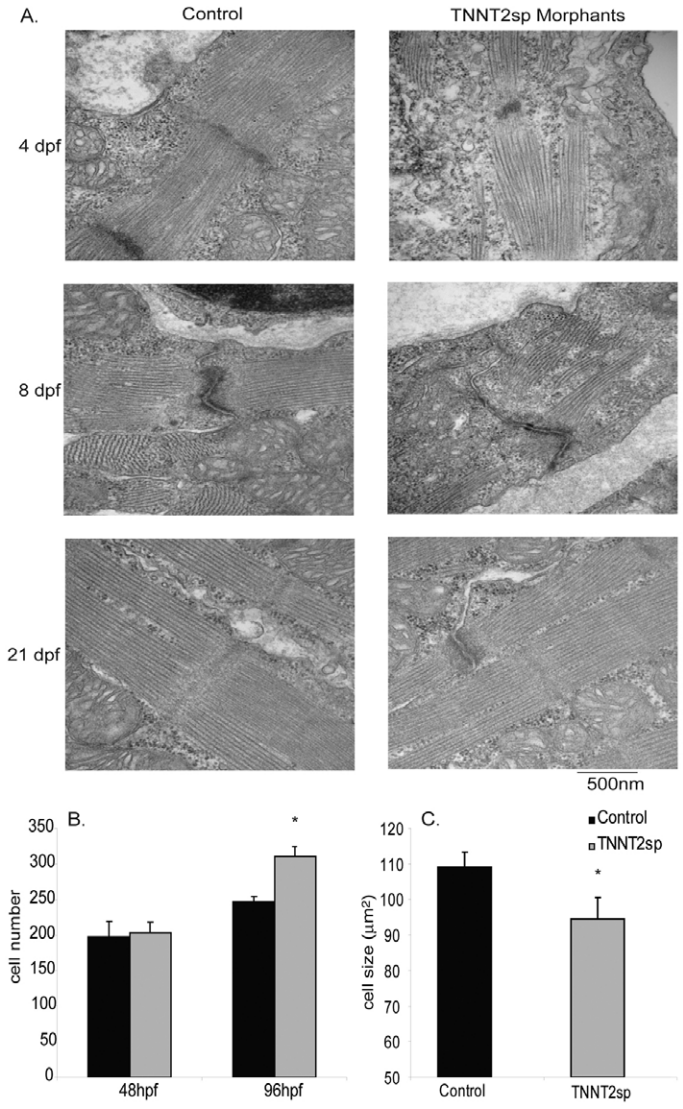

Fig. 3. Disruption of sarcomere structure and induction of myocardial hyperplasia in TNNT2sp morphants. (A) Representative electron micrographs of 96 hpf (top), 8 dpf (middle) and 21 dpf (bottom) ventricular cardiomyocytes. (B) Total cardiomyocytes at 48 hpf and 96 hpf. (C) Cardiomyocyte area at 96 hpf. *P<0.05; n=3-5 hearts per time point. All data expressed as mean + s.e.m.

(P-MAGE) (Kim et al., 2007). The mouse ventricular tissue that was analyzed was harvested from alphaMHC403 heterozygote mice. These mice harbor a missense mutation in their alpha myosin heavy chain gene (*myh6*) that causes a change from arginine to glutamine at position 403 (Geisterfer-Lowrance et al., 1996). The expression of 122 genes was significantly changed in both our *tnnt2* morphant zebrafish dataset and the mouse alphaMHC403 HCM P-MAGE dataset. Of these genes, 74 were regulated in a concordant fashion and 48 were regulated in a discordant fashion (cumulative binomial probability=0.012) (Fig. 6). Induction of the natriuretic peptide gene *nppa* and multiple genes encoding Ca^{2+} regulatory proteins was seen in both datasets (*casq2*, *cast* and *srl*). In addition, there was concordant downregulation of a number of genes important to cardiovascular biology (*abcc9*, *foxo1* and *hey1*).

DISCUSSION

Our embryonic zebrafish model of a human sarcomeric gene mutation recapitulated many of the cellular and transcriptional responses seen in adult organisms with these mutations. In the context of a hypertrophic stimulus, even the initial embryonic cardiomyocytes exhibited sarcomeric disarray, a hallmark of sarcomeric gene mutations in humans and mammalian models. These cellular phenomena were accompanied by a robust transcriptional response closely paralleling the patterns of gene expression observed in a murine model of HCM. In addition, there was a significant perturbation of cardiomyocyte Ca^{2+} handling evident during cardiogenesis in this zebrafish model. Despite these similarities with adult HCM models, the embryonic zebrafish heart did not display cardiomyocyte hypertrophy in response to this sarcomeric mutation, but rather developed significant cardiomyocyte hyperplasia.

The recapitulation of this human TNNT2 splicing abnormality has dramatic effects on early cardiomyocyte sarcomerogenesis, and these seem to be reversible in the embryonic heart. Interestingly, the disruption in sarcomerogenesis persisted for a considerable period (several days) after the abnormal *tnnt2* splice product was eliminated but, by 21 dpf, the sarcomere had fully remodeled and normal sarcomerogenesis was evident. These observations suggest that even the profound abnormalities of sarcomeric structure seen in human cardiomyopathic cells might be reversible if the genetic mutation can be 'silenced' through chemical or genetic means. Nevertheless, the sarcomere recovery that we have observed in morphant embryos might reflect distinctive characteristics of the zebrafish embryonic heart, and post-natal mammalian sarcomeres might not be so plastic. Indeed, recent data in a rabbit model of HCM suggest that, although chemical modifiers might be able to reverse the interstitial fibrosis and cardiomyocyte hypertrophy associated with longstanding HCM, they do not modify myocyte disarray (Lombardi et al., 2009).

Despite the phylogenetic distance between zebrafish and mammals, there is substantial conservation of the gene expression responses to sarcomeric gene mutations. One of the most highly upregulated genes in the TNNT2sp morphant embryos is *nppa*. This induction of the natriuretic peptide pathway is a consistent feature of mammalian models of HCM and acquired hypertrophy. There was robust correlation of gene expression in our morphant with published cardiac gene expression analysis in an adult mouse HCM model across multiple pathways. The transcriptional effects seen in our zebrafish embryos were evident despite the potential limitations of whole-embryo expression profiling. These data highlight the fundamental nature of the hypertrophic transcriptional program, which is activated virtually from the onset of cardiac function in this zebrafish model of HCM.

One advantage of whole-embryo expression profiling is that systemic responses to cardiac-restricted stimuli can be assessed. Developing an understanding of how the whole organism responds to altered cardiac function could provide useful insights into the pathophysiology of hypertrophy and the factors determining progression to the systemic syndrome of congestive heart failure. Comprehensive pathway analyses of gene expression in our

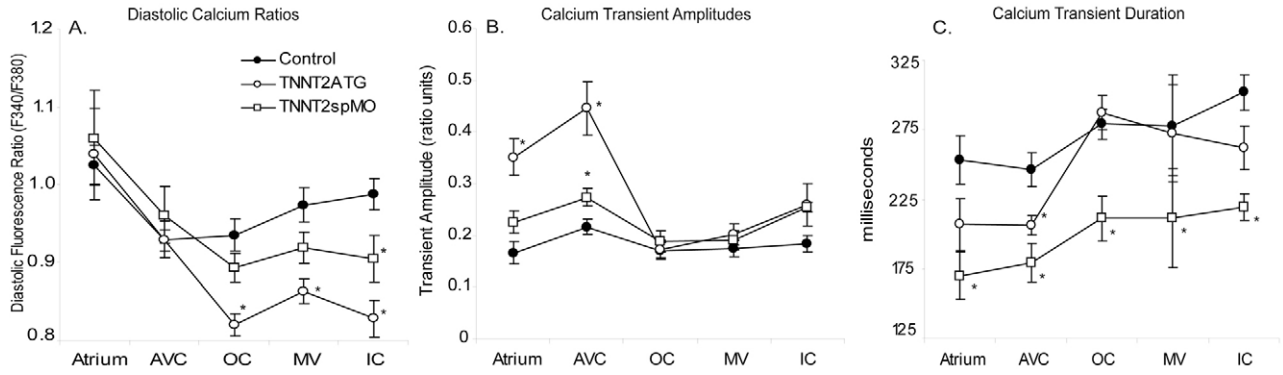

Fig. 4. Distinct alterations in Ca^{2+} handling induced by altered TNNT2 splicing. Diastolic (A) and transient amplitude (B) Ca^{2+} measurements in specific heart regions in controls, TNNT2sp morphants and TNNTatg (null) morphants. (C) CTD50 measured in atrium, atrioventricular canal (AVC), outer ventricular curvature (OC), mid-ventricle (MV) and inner ventricular curvature (IC). Asterisk donates $P<0.05$ for comparison of TNNT2sp morphant with control sample, or TNNT2atg morphant with control. All data expressed as mean ± s.e.m.

embryonic zebrafish TNNT2sp model demonstrated downregulation of a group of hormonal genes. Interestingly, these same neuroendocrine genes have been shown to modify cardiomyocyte survival (*ghrh* and *pth1a*) (Cha et al., 2009; Granata et al., 2009), directly modulate the cardiomyocyte hypertrophic response (*uts2*) (Tzanidis et al., 2003) or are transcriptionally regulated by hypertrophic pathways (*pomca*) (Chalmers et al., 2008).

Another aspect of the pleiotropy of HCM is the variable risk of cardiac arrhythmias. In animal models of HCM, arrhythmias can develop before significant fibrosis occurs, suggesting that primary alterations in cardiomyocyte electrical properties, in addition to

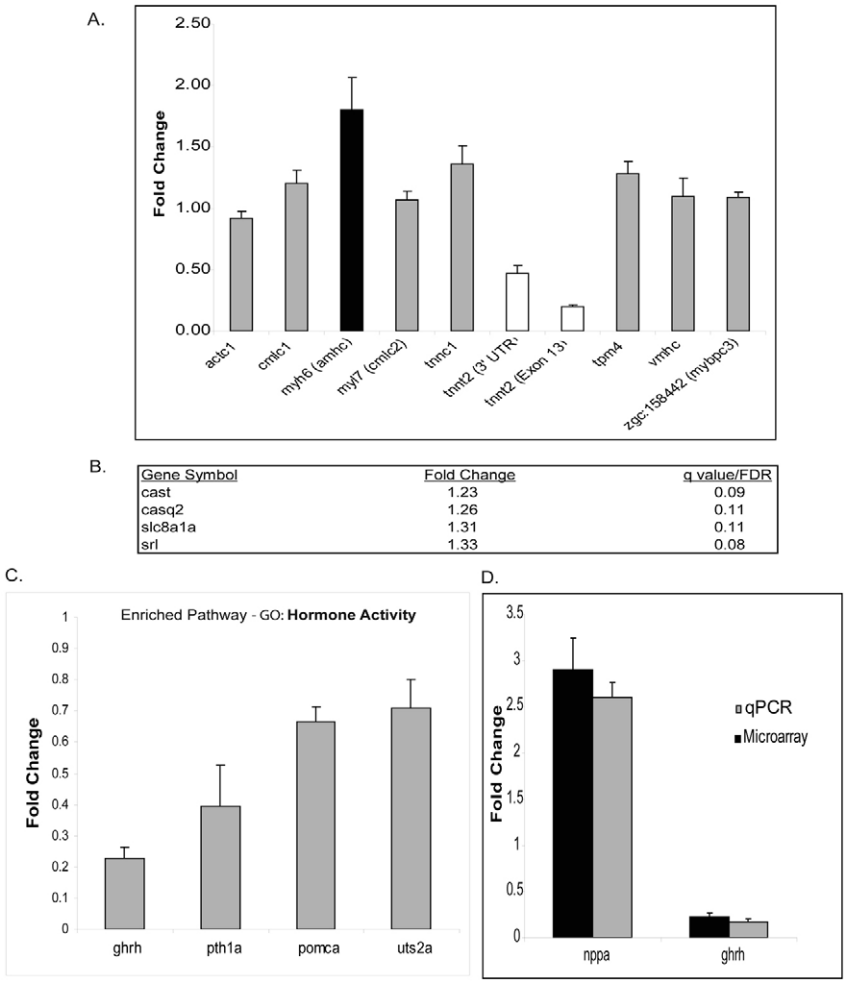

Fig. 5. Altered *tnnt2* splicing induces significant changes in the expression of sarcomeric genes, neurohormonal genes and markers of hypertrophy. (A) Expression profiling identifies upregulation of *myh6* (black bar) and confirms efficacy of TNNT2sp MO [white bar labeled 'tnnt2 (Exon 13)'. (B) Genes involved in cardiomyocyte Ca^{2+} handling that are differentially regulated in TNNT2sp morphants. (C) Pathway analysis identifies significant downregulation of expression of genes encoding specific hormones – *ghrh*, *pth1a*, *pomca* and *uts2a*. (D) qPCR confirmation of select up- and downregulated genes. All data expressed as mean + s.e.m.

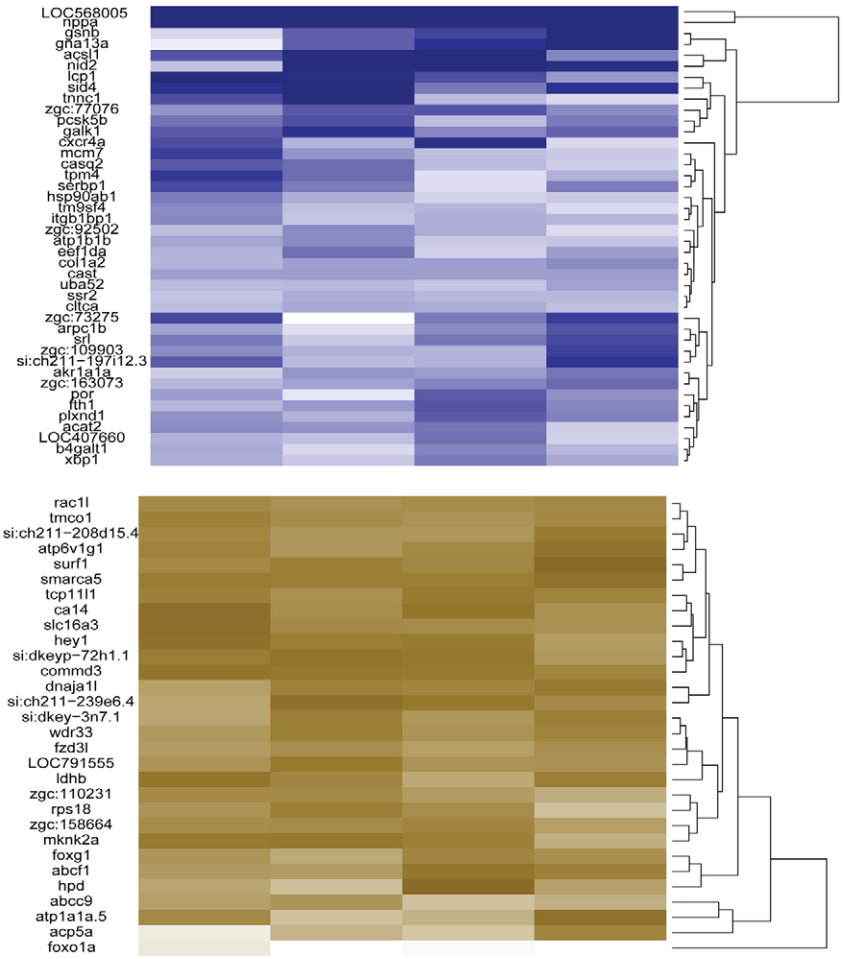

Fig. 6. Conservation of gene expression between the zebrafish and mouse models of sarcomeric protein mutations. The zebrafish genes that were concordantly upregulated (blue) or downregulated (brown) compared with a mouse model of HCM are displayed in a heatmap. Top – most upregulated gene; bottom – most downregulated gene. Each column corresponds to a unique biological replicate.

fibrotic scarring, underlie the arrhythmogenesis (Baudenbacher et al., 2008; Wolf et al., 2005). Our TNNT2sp morphants had significant shortening of CTD50 in both atrium and ventricle. Interestingly, complete loss of Tnnt2 resulted in distinctive effects on diastolic Ca^{2+} concentrations and on the amplitude of the Ca^{2+} transient. These differences suggest that competing effects on Ca^{2+} handling result from the deletion of different domains within Tnnt2, and these non-overlapping roles might explain the disparate effects of individual troponin mutations on Ca^{2+} sensitivity in vitro (Szczesna et al., 2000). Among the potential mechanisms for the reduced CTD50 observed in the TNNT2sp morphants are effects on sarcomeric buffering of cytoplasmic Ca^{2+} or the upregulation of a number of Ca^{2+} handling proteins – *slc8a1a*, *casq2* and *srl*. Increased expression of *slc8a1a* and the sarcoplasmic reticulum (SR) genes *casq2* and *srl* would facilitate extrusion of Ca^{2+} from the cytoplasm to the extracellular space or SR, respectively (Harris et al., 2006; Kubalova et al., 2004; Yoshida et al., 2005). The role of *cast* is less clear, but it has been shown to bind and modulate the activity of Cav1.2, the cardiac L-type calcium channel (Hao et al., 2000). The precise mechanisms by which reduction in CTD50 might result in arrhythmogenesis are not known. However, abnormalities in CTD50 are seen in animal models of catecholaminergic polymorphic ventricular tachycardia (CPVT) (Song et al., 2007).

Cellular hypertrophy is a fundamental response of the stressed heart. Many of the pathways associated with cell division are known to be activated in this hypertrophic response, leading to the hypothesis that cardiomyocyte hypertrophy might be the result of a fundamental block in karyokinesis and cytokinesis, by which the adult cardiomyocyte is unable to disassemble sarcomeres, uncouple from neighboring cells and divide (Ahuja et al., 2007). Nuclear division and polyploidy are observed in the latest stages of human heart failure and reverse with ventricular unloading, but cellular dynamics earlier in the pathophysiological cascade have not yet been explored (Rivello et al., 2001). In the zebrafish model that we generated, we were able to explore the effects of disrupted sarcomere gene function during cardiogenesis. We found that when the embryonic heart is exposed to a hypertrophic stimulus, in contrast to the response in the adult mammalian heart, a hyperplastic response occurs. Whereas pressure or volume overload seem to increase cardiomyocyte proliferation in the fetal mammalian heart, the effects of such hypertrophic stimuli on the relevant molecular pathways have not been identified (Saiki et al., 1997; Sedmera et al., 2003). We were able to show that, despite the hyperplastic nature of the embryonic response to a primary hypertrophic stimulus, the classic hypertrophic transcriptional stress response networks are activated in this zebrafish model. Cross-species comparison of the distinctive molecular networks

regulating cardiomyocyte hypertrophy and hyperplasia could offer insights into the factors determining these differential responses to a single stimulus.

It is interesting to compare our findings with those in a murine model with transgenic overexpression of a comparable truncated TNNT2 protein under the control of the *alphaMHC(myh6)* promoter (Tardiff et al., 1998). In both fish and mouse there was evidence of reduced ventricular chamber dimensions and some impairment of contractile function. In the transgenic mouse there was evidence of reduced cell number, but in the fish we observed increased cell number, despite the reduction in chamber dimensions, with a parallel reduction in cell size. Importantly, this particular transgenic mouse model did not exhibit evidence of induction of the typical transcriptional markers of the hypertrophic response, unlike other vertebrate cardiac troponin T models (Tardiff et al., 1999). It remains to be seen whether these differences between mouse and fish models result from the onset of mutant allele expression in different time windows (the *alphaMHC* promoter does not become active until late in cardiac development), or from intrinsic differences between murine and zebrafish cardiomyocytes.

Although zebrafish models of complete loss of TNNT2 or truncation of the TNNT2 protein exist, we designed our approach to precisely recapitulate a known human sarcomeric gene mutation while maintaining comprehensive native regulation and wild-type hemizygous gene dose. Zebrafish homozygous for a null *tnnt2* mutation (*silent heart*), with severe truncation of Tnnt2 protein or lack of translation, develop ultrastructural characteristics of HCM, mainly sarcomeric disarray. However, these recessive zebrafish *tnnt2* mutants, as well as the cognate homozygous *tnnt2*-null mouse, never exhibit myocardial contraction (Sehnert et al., 2002; Ahmad et al., 2008). Similarly, C-terminal truncations of zebrafish *tnnt2* (exclusion of exon 12; see supplementary material Fig. S1 for exon numbering) almost completely abolish myocardial contraction and are associated with a total loss of wild-type *tnnt2* transcript (Huang et al., 2009). We sought to model a dominant human *tnnt2* mutation, avoiding the non-physiological elimination of contractile function and its resultant effects on cardiogenesis.

In conclusion, recapitulation of human hypertrophic cardiomyopathy gene mutations in the zebrafish facilitates access to the earliest effects of these genetic perturbations. We were able to confirm the primary defects in sarcomere assembly and establish the activation of a subset of hypertrophic pathways as well as the presence of abnormal Ca^{2+} handling during initial cardiogenesis. We also obtained definitive evidence for a hyperplastic cardiomyocyte response to a genetic hypertrophic stimulus during development. Although this might simply reflect the plastic environment of the embryo or a general property of the zebrafish heart, it will be important to re-evaluate the role of regional perturbations in cell number in the unique features of HCM, such as asymmetric septal hypertrophy. In addition, understanding the comparative biology of hyperplastic and hypertrophic responses across a range of species may inform efforts to manipulate terminally differentiated cardiomyocytes or cardiac progenitor cell populations in human disease. Ultimately, our work suggests that the pleiotropy of human hypertrophic cardiomyopathy may be influenced by selection pressures exerted during development.

METHODS

The investigation conforms to the Guide for the Care and Use of Laboratory Animals published by the US National Institutes of Health (NIH Publication No. 85-23, revised 1996).

Morpholino injection

Morpholinos (Gene Tools, LLC, Philomath, OR) were resuspended in 1× Danieu's solution and 5 ng injected into fertilized eggs from TuAB fish at the single-cell stage. The *tnnt2* exon 13 splice (TNNT2sp) MO sequence was: 5′-TAGACACAGATGAACT-CACAATTTC-3′. There is a polymorphism at the morpholino-binding site in exon 13 that is highlighted in red in supplementary material Fig. S1. The 5 bp mismatch control morpholino sequence was (base changes are lower case): 5′-TAcACAgAGATcAACTCA-gAATaTC-3′. To determine whether the morpholino altered splicing of the *tnnt2* mRNA, we designed primers that flanked *tnnt2* exon 13 and then performed RT-PCR. Primer sequences are TNNT2ex11F: 5′-AGAAGAAGATTCTCGGTGATCG-3′ and TNNT2ex14R: 5′-CAACAGTGGTCAGCTCCTCTC-3′. We sequenced the PCR product to confirm that exon 13 was completely excluded. The TNNT2atg ('silent heart') morpholino sequence is 5′-CATGTTTGCTCTGATCTGACACGCA-3′ (Sehnert et al., 2002).

Electron microscopy

Embryos were fixed at 96 hpf, 8 dpf and 21 dpf, embedded in Epon 812 (Polysciences) and sectioned. Thin sections were cut on a Reichert Ultracut E ultramicrotome and collected onto Formar-coated slot grids. Sections were post-stained with uranyl acetate and lead citrate, and viewed in a Philips CM10 electron microscope at 80 keV.

Myocardial function

Embryos were laterally positioned and allowed to acclimate. Video microscopy was performed with an Axioplan (Zeiss) upright microscope and 544 frames were digitally captured at identical levels of magnification (10×) and frame rate (250 frames per second). Sequential still frames were analyzed to identify ESD and EDD. FS was calculated using the formula (EDD − ESD)/(EDD).

Cardiomyocyte quantification

cmlc2::DsRed-nuc embryos were injected with control or TNNT2sp MO at the one-cell stage. At 48 or 96 hpf the embryos were euthanized and fixed in 4% PFA for 12 hours at 4°C. The embryos were transferred to PBS and stored at 4°C. Whole embryos were mounted in 1% low-melt agar and were imaged using a Zeiss LSM5 Pascal confocal microscope and 40× water-immersion lens. *z*-stack images were collected and a three-dimensional image projection was created using ImageJ (NIH). DsRed-positive nuclei were then counted using ImageJ software.

Cell size measurement

Control and TNNT2sp morphant embryos were euthanized and fixed in 4% PFA for 12 hours at 4°C. They were then transferred to 100% methanol and stored at −20°C. The embryos were then rehydrated in PBST. After rehydration, the embryos were washed in a blocking buffer (2 mg/ml BSA, 2% goat serum, 1% DMSO in PBST) for 2 hours at 25°C. They were then incubated with mouse

anti-ZN8 (binds to ventricular cardiomyocyte cell surface) [Developmental Studies Hybridoma Bank (DSHB); 1:50] at 4°C for 12 hours, and then with Alexa Fluor 546 (Invitrogen; 1:1000) for 3 hours at 25°C. Whole embryos were mounted in 1% low-melt agar and were imaged using a Zeiss LSM5 Pascal confocal microscope and 40× water-immersion lens. ImageJ analysis software was used to measure the cell surface area of control and TNNT2sp morphant cardiomyocytes.

Ca^{2+} imaging

Hearts were isolated from zebrafish embryos at 72 hpf and placed in normal Tyrode's solution (NT), which contained (in mM) Na^+ (136), K^+ (5.4), Mg^{2+} (1.0), PO_4^{3-} (0.3), Ca^{2+} (1.8), glucose (5.0) and HEPES (10.0) at pH 7.4. The chamber was mounted on the stage of an inverted microscope (TE-2000, Nikon). Excitation light was generated by a 120 W metal halide lamp (X-Cite 120, Exfo), transmitted through a 525/50 nm excitation filter and reflected onto the preparation by a 560-nm-cutoff dichroic mirror. Fluorescence emission was passed through a 635 nm long-pass emission filter and reflected by a mirror towards the camera, which was mounted at a side-port. For ratiometric Ca^{2+} transient recordings, hearts were loaded for 15 minutes with 50 μM of the Ca^{2+}-sensitive dye Fura-2, AM (Invitrogen). Hearts were then incubated in NT solution at room temperature for 30-45 minutes to allow complete intracellular hydrolysis of the esterified dye and placed in a perfusion bath (Warner Instruments) that contained NT solution supplemented with 30 μM of the excitation-contraction uncoupler blebbistatin (Calbiochem) to inhibit motion. A high-speed monochromator (Optoscan, Cairn Research, UK) was used to rapidly switch the excitation wavelength between 340 nm and 380 nm with a bandwidth of 20 nm and at a rate of 500 $second^{-1}$. Wavelength switching was synchronized with the camera to ensure that fluorescence acquisition occurred at well-defined time intervals, i.e. when the monochromator had reached the two target wavelengths. Each ratio acquisition required four frames, thus resulting in a final ratio rate of 125 $second^{-1}$. The excitation light was reflected by a 400-nm-cutoff dichroic mirror and fluorescence emission was collected by the camera through a 510/80 nm emission filter. For the measurement of fluorescence intensities, a high-speed 80×80-pixel CCD camera (CardioCCD-SMQ, RedShirtImaging, LLC) with 14-bit resolution was used. Using a 20×/0.75 NA objective and a 0.5× C-mount adapter, the final magnification was 10×, resulting in a pixel-to-pixel distance of 2.2 μm.

Fluorescence data signal processing and Ca^{2+} transient analysis

Acquired fluorescence images were exported as TIFF stacks and analyzed using Matlab (Mathworks) software. Regions of interest (ROIs) 16×16 pixels in size, covering an area of about 35×35 μm of epicardial tissue, were defined within the atrium, atrioventricular junction, and the inner curvature (IC) and the outer curvature (OC) of the ventricle. The size of the ROI was the same for all measurements. Errors resulting from variations in the positions of these ROIs within each target area (e.g. atrium, ventricle) of the same heart were less than 10% and smaller than the naturally occurring variations of Ca^{2+} concentrations between different hearts of the same genotype. Individual Ca^{2+} transients were extracted from each pixel contained within each ROI to calculate minimum (diastolic) and maximum (systolic) fluorescence ratios. Ca^{2+} transient amplitude was defined as the difference between the systolic and diastolic ratios, and transient duration (CTD50) as the time difference between the upstroke and the decay phases, measured at 50% of the amplitude. Diastolic ratios, transient amplitudes and transient durations were calculated and measurements averaged for all pixels within each ROI.

Gene expression analysis

Control- and TNNT2sp-MO-injected embryos were collected at 96 hpf in groups of 40 embryos, and RNA was extracted using Trizol (Invitrogen) and further purified with RNeasy columns (Qiagen). Four biological replicates of control and TNNT2sp embryos were then analyzed using a two-color zebrafish-specific microarray (Agilent). Primary microarray data files and matrix files are available at NIH GEO repository – GSE20179.

All statistical analysis was performed using the R software package (2.9.2; www.cran.r-project.org). Agilent two-color microarray data were analyzed using the limma package. Limma employs a generalized linear model with empirical Bayesian methods to 'borrow information' across genes for more stable estimates of significance and magnitude of change, especially when the number of arrays is small. Unadjusted *P*-values for association were input into the fdrtool package for empirical tail-based false discovery rate (FDR) calculation (Strimmer, 2008). An arbitrary FDR threshold of 0.15 was selected – at this threshold, we expect that >85% of the 'significant' probe sets represent true positives. We have found that these relaxed thresholds combined with further pathway analysis methods can be useful for identifying enriched pathways. The FuncAssociate program was used for examining GO term enrichment (supplementary material Table S2).

A previously published hypertrophic cardiomyopathy P-MAGE data set (all tags significant at P=0.05) was downloaded for comparison of significantly changed orthologs (Kim et al., 2007). Mouse orthologs for zebrafish genes were identified using a combination of the Inparanoid, Zfin and Ensembl (www.ensembl.org) databases (Ostlund et al., 2010; Sprague et al., 2008). An additional number of orthologs were identified by matching symbol names and performing bidirectional BLASTN to ensure that the corresponding ortholog represented the top BLAST hit in each case. A total of 122 orthologs were significant at P=0.05 (P-MAGE) and the FDR was 0.15 (zebrafish array). We compared the direction of change for each of these and found 74 that demonstrated concordant change. Statistical significance was assessed as follows. Under the null model, we would expect a 50% probability for the concordance for any given pair of orthologs. The probability that 74 or more of these 122 orthologs are concordant is thus given by the cumulative binomial distribution with n=122 and P=0.5, analogous to the probability of 74 heads in 122 flips of a fair coin. To identify similarities in patterns of change for different probe sets, the limma coefficients for the 74 probe sets with concordant change in the P-MAGE and microarray data sets were depicted in a heatmap, using the heatmap function in R.

FuncAssociate uses a hypergeometric test and correction for multiple hypothesis testing to formally evaluate statistical

TRANSLATIONAL IMPACT

Clinical issue

Hypertrophic cardiomyopathy (HCM) is one of the most common monogenic cardiovascular disorders, affecting approximately 1 in every 500 individuals. The disease is characterized by increased ventricular wall thickness, myocyte disarray and an increased risk of sudden cardiac death. Most of the mutations that cause this disease affect genes encoding cardiac sarcomeric contractile proteins such as cardiac troponin T (TNNT2). However, although the underlying genetic causes have been identified, the fact that there is substantial phenotypic variation among family members harboring identical mutations suggests that the disease is also influenced by environmental or genetic modifiers.

Results

To examine the effect of an HCM-associated mutation during cardiac development, and to identify unknown modifiers of HCM, the authors of this study created a zebrafish morphant of *tnnt2* and examined embryonic cardiac development. Analysis of sarcomere organization and gene expression profiling indicated that the cardiac pathology in zebrafish *tnnt2* morphant embryos is similar in many respects to humans with HCM and also to mouse models of the disease. However, rather than developing cardiomyocyte hypertrophy as observed in HCM, zebrafish *tnnt2* morphant embryos exhibited a hyperplastic myocardial response. The authors also identified unique alterations in cardiomyocyte Ca^{2+} handling that occur during the earliest stages of heart development and are secondary to the *tnnt2* mutation. This suggests that perturbations in cardiomyocyte Ca^{2+} handling seen in HCM might occur quite early in the disease process, before the overt pathological changes have taken place.

Implications and future directions

These findings indicate that a sarcomeric gene mutation associated with HCM in humans has a significant influence on early cardiogenesis in the zebrafish embryo. This suggests that the disease phenotype in adult humans might result from cumulative effects of long-standing perturbations in cardiomyocyte biology that begin at the earliest stages of heart development. In addition, the unique biological responses of the embryonic heart to sarcomeric gene mutations might alter the final pathological characteristics of the adult disease. Potential therapeutic manipulation of these pathological processes might need to be performed at the earliest stages of the disease process, before many of the typical clinical manifestations of the disease develop.

significance for pathway enrichment (Berriz et al., 2009). Upregulated and downregulated genes were analyzed separately and ranked by magnitude of change. For some genes, multiple probe sets were available, usually with differing magnitude and significance of change. We operated under the assumption that differing effect sizes for multiple probe sets arises from some combination of chance variation in probe binding efficiencies, differential regulation of individual isoforms and measurement error. Because a single probe set had to be selected for subsequent analyses, for those genes mapping to multiple probe sets, the probe set with the lowest *P*-value was selected, thus making the optimistic assumption that the lowest *P*-value was capturing the true, maximal change in response to the perturbation. Although this assumption might introduce noise in further analyses, it should not introduce any systematic bias in terms of direction of change.

qPCR was performed using RNA extracted from whole embryos using Trizol reagent (Invitrogen) and reverse transcribed with the QuantiTect Reverse Transcription Kit (Qiagen). Gene-specific primers and SYBR Green reagent (Applied Biosystems) were used to perform the PCR portion of the experiment. The $\Delta\Delta C_t$ method was used to normalize the gene of interest to the endogenous housekeeping gene *Rpl13alpha*. Then the experimental sample was divided by the control sample to determine the level of induction. qPCR primer sequences: nppa: F 5′-GATGTACAAGCGC-ACACGTT-3′, R 5′-TCTGATGCCTCTTCTGTTGC-3′; ghrh: F 5′-AGACTTGGACCAGAAACTGAAAGC-3′, R 5′-TGTGGGT-CTCTGTAACTTTGTTCA-3′; 13alpha: F 5′-TCTGGAGGACT-GTAAGAGGTATGC-3′, R 5′-AGACGCACAATCTTGAGAG-CAG-3′.

Statistics

To compare two continuous variables a Student's *t*-test was used for normally distributed data. For data that were not normally distributed, a Wilcoxon rank-sum test was used. All data are expressed as mean ± s.e.m., unless otherwise noted.

ACKNOWLEDGEMENTS

We would like to thank Mary McKee for the electron microscopy technical assistance and Jennifer Love for the microarray technical assistance. We would also like to thank Michael Fifer and Barry London for their advice and encouragement. This work was supported by an institutional grant from the Hypertrophic Cardiomyopathy Center at Massachusetts General Hospital (C.A.M.) and T32HL007208 (J.R.B., R.C.D.).

COMPETING INTERESTS

The authors declare that they do not have any competing or financial interests.

AUTHOR CONTRIBUTIONS

J.R.B. and C.A.M. conceived and designed the experiments. J.R.B., D.P. and S.C. performed the experiments. J.R.B., R.C.D., A.A.W. and C.A.M. analyzed the data. J.R.B. and C.A.M. wrote the paper.

SUPPLEMENTARY MATERIAL

Supplementary material for this article is available at http://dmm.biologists.org/lookup/suppl/doi:10.1242/dmm.006148/-/DC1

REFERENCES

Ahmad, F., Banerjee, S. K., Lage, M. L., Huang, X. N., Smith, S. H., Saba, S., Rager, J., Conner, D. A., Janczewski, A. M., Tobita, K. et al. (2008). The role of cardiac troponin T quantity and function in cardiac development and dilated cardiomyopathy. *PLoS ONE* **3**, e2642.

Ahuja, P., Sdek, P. and MacLellan, W. R. (2007). Cardiac myocyte cell cycle control in development, disease, and regeneration. *Physiol. Rev.* **87**, 521-544.

Alcalai, R., Seidman, J. G. and Seidman, C. E. (2007). Genetic basis of hypertrophic cardiomyopathy: from bench to the clinics. *J. Cardiovasc. Electrophysiol.* **19**, 104-110.

Arad, M., Seidman, J. G. and Seidman, C. E. (2002). Phenotypic diversity in hypertrophic cardiomyopathy. *Hum. Mol. Genet.* **11**, 2499-2506.

Baudenbacher, F., Schober, T., Pinto, J. R., Sidorov, V. Y., Hilliard, F., Solaro, R. J., Potter, J. D. and Knollmann, B. C. (2008). Myofilament Ca2+ sensitization causes susceptibility to cardiac arrhythmia in mice. *J. Clin. Invest.* **118**, 3893-3903.

Berriz, G. F., Beaver, J. E., Cenik, C., Tasan, M. and Roth, F. P. (2009). Next generation software for functional trend analysis. *Bioinformatics* **25**, 3043-3044.

Berriz, G. F., King, O. D., Bryant, B., Sander, C. and Roth, F. P. (2003). Characterizing gene sets with FuncAssociate. *Bioinformatics* **19**, 2502-2504.

Cha, H., Jeong, H. J., Jang, S. P., Kim, J. Y., Yang, D. K., Oh, J. G. and Park, W. J. (2009). PTH accelerates decompensation following left ventricular hypertrophy. *Exp. Mol. Med.* **42**, 61-61.

Chalmers, J. A., Lin, S. Y., Martino, T. A., Arab, S., Liu, P., Husain, M., Sole, M. J. and Belsham, D. D. (2008). Diurnal profiling of neuroendocrine genes in murine heart, and shift in proopiomelanocortin gene expression with pressure-overload cardiac hypertrophy. *J. Mol. Endocrinol.* **41**, 117-124.

Geisterfer-Lowrance, A. A., Christe, M., Conner, D. A., Ingwall, J. S., Schoen, F. J., Seidman, C. E. and Seidman, J. G. (1996). A mouse model of familial hypertrophic cardiomyopathy. *Science* **272**, 731-734.

Granata, R., Trovato, L., Gallo, M. P., Destefanis, S., Settanni, F., Scarlatti, F., Brero, A., Ramella, R., Volante, M., Isgaard, J. et al. (2009). Growth hormone-releasing hormone promotes survival of cardiac myocytes in vitro and protects against ischaemia-reperfusion injury in rat heart. *Cardiovasc. Res.* **83**, 303-312.

Hao, L. Y., Kameyama, A., Kuroki, S., Takano, J., Takano, E., Maki, M. and Kameyama, M. (2000). Calpastatin domain L is involved in the regulation of L-type

Ca2+ channels in guinea pig cardiac myocytes. *Biochem. Biophys. Res. Commun.* **279**, 756-761.

Harris, K. M., Spirito, P., Maron, M. S., Zenovich, A. G., Formisano, F., Lesser, J. R., Mackey-Bojack, S., Manning, W. J., Udelson, J. E. and Maron, B. J. (2006). Prevalence, clinical profile, and significance of left ventricular remodeling in the end-stage phase of hypertrophic cardiomyopathy. *Circulation* **114**, 216-225.

Huang, W., Zhang, R. and Xu, X. (2009). Myofibrillogenesis in the developing zebrafish heart: A functional study of tnnt2. *Dev. Biol.* **331**, 237-249.

Kim, J. B., Porreca, G. J., Song, L., Greenway, S. C., Gorham, J. M., Church, G. M., Seidman, C. E. and Seidman, J. G. (2007). Polony multiplex analysis of gene expression (PMAGE) in mouse hypertrophic cardiomyopathy. *Science* **316**, 1481-1484.

Knollmann, B. C., Kirchhof, P., Sirenko, S. G., Degen, H., Greene, A. E., Schober, T., Mackow, J. C., Fabritz, L., Potter, J. D. and Morad, M. (2003). Familial hypertrophic cardiomyopathy-linked mutant troponin T causes stress-induced ventricular tachycardia and Ca2+-dependent action potential remodeling. *Circ. Res.* **92**, 428-436.

Kubalova, Z., Gyorke, I., Terentyeva, R., Viatchenko-Karpinski, S., Terentyev, D., Williams, S. C. and Gyorke, S. (2004). Modulation of cytosolic and intra-sarcoplasmic reticulum calcium waves by calsequestrin in rat cardiac myocytes. *J. Physiol.* **561**, 515-524.

Lombardi, R., Rodriguez, G., Chen, S. N., Ripplinger, C. M., Li, W., Chen, J., Willerson, J. T., Betocchi, S., Wickline, S. A., Efimov, I. R. et al. (2009). Resolution of established cardiac hypertrophy and fibrosis and prevention of systolic dysfunction in a transgenic rabbit model of human cardiomyopathy through thiol-sensitive mechanisms. *Circulation* **119**, 1398-1407.

Mably, J. D., Mohideen, M. A., Burns, C. G., Chen, J. N. and Fishman, M. C. (2003). heart of glass regulates the concentric growth of the heart in zebrafish. *Curr. Biol.* **13**, 2138-2147.

Ostlund, G., Schmitt, T., Forslund, K., Kostler, T., Messina, D. N., Roopra, S., Frings, O. and Sonnhammer, E. L. (2010). InParanoid 7, new algorithms and tools for eukaryotic orthology analysis. *Nucleic Acids Res.* **38**, D196-D203.

Rivello, H. G., Meckert, P. C., Vigliano, C., Favaloro, R. and Laguens, R. P. (2001). Cardiac myocyte nuclear size and ploidy status decrease after mechanical support. *Cardiovasc. Pathol.* **10**, 53-57.

Saiki, Y., Konig, A., Waddell, J. and Rebeyka, I. M. (1997). Hemodynamic alteration by fetal surgery accelerates myocyte proliferation in fetal guinea pig hearts. *Surgery* **122**, 412-419.

Sedmera, D., Thompson, R. P. and Kolar, F. (2003). Effect of increased pressure loading on heart growth in neonatal rats. *J. Mol. Cell. Cardiol.* **35**, 301-309.

Sehnert, A. J., Huq, A., Weinstein, B. M., Walker, C., Fishman, M. and Stainier, D. Y. (2002). Cardiac troponin T is essential in sarcomere assembly and cardiac contractility. *Nat. Genet.* **31**, 106-110.

Seidman, J. G. and Seidman, C. (2001). The genetic basis for cardiomyopathy: from mutation identification to mechanistic paradigms. *Cell* **104**, 557-567.

Song, L., Alcalai, R., Arad, M., Wolf, C. M., Toka, O., Conner, D. A., Berul, C. I., Eldar, M., Seidman, C. E. and Seidman, J. G. (2007). Calsequestrin 2 (CASQ2) mutations increase expression of calreticulin and ryanodine receptors, causing catecholaminergic polymorphic ventricular tachycardia. *J. Clin. Invest.* **117**, 1814-1823.

Sprague, J., Bayraktaroglu, L., Bradford, Y., Conlin, T., Dunn, N., Fashena, D., Frazer, K., Haendel, M., Howe, D. G., Knight, J. et al. (2008). The Zebrafish Information Network: the zebrafish model organism database provides expanded support for genotypes and phenotypes. *Nucleic Acids Res.* **36**, D768-D772.

Strimmer, K. (2008). fdrtool: a versatile R package for estimating local and tail area-based false discovery rates. *Bioinformatics* **24**, 1461-1462.

Szczesna, D., Zhang, R., Zhao, J., Jones, M., Guzman, G. and Potter, J. D. (2000). Altered regulation of cardiac muscle contraction by troponin T mutations that cause familial hypertrophic cardiomyopathy. *J. Biol. Chem.* **275**, 624-630.

Tardiff, J. C., Factor, S. M., Tompkins, B. D., Hewett, T. E., Palmer, B. M., Moore, R. L., Schwartz, S., Robbins, J. and Leinwand, L. A. (1998). A truncated cardiac troponin T molecule in transgenic mice suggests multiple cellular mechanisms for familial hypertrophic cardiomyopathy. *J. Clin. Invest.* **101**, 2800-2811.

Tardiff, J. C., Hewett, T. E., Palmer, B. M., Olsson, C., Factor, S. M., Moore, R. L., Robbins, J. and Leinwand, L. A. (1999). Cardiac troponin T mutations result in allele-specific phenotypes in a mouse model for hypertrophic cardiomyopathy. *J. Clin. Invest.* **104**, 469-481.

Thierfelder, L., Watkins, H., MacRae, C., Lamas, R., McKenna, W., Vosberg, H. P., Seidman, J. G. and Seidman, C. E. (1994). Alpha-tropomyosin and cardiac troponin T mutations cause familial hypertrophic cardiomyopathy: a disease of the sarcomere. *Cell* **77**, 701-712.

Tzanidis, A., Hannan, R. D., Thomas, W. G., Onan, D., Autelitano, D. J., See, F., Kelly, D. J., Gilbert, R. E. and Krum, H. (2003). Direct actions of urotensin II on the heart: implications for cardiac fibrosis and hypertrophy. *Circ. Res.* **93**, 246-253.

Wagner, K. D., Wagner, N., Ghanbarian, H., Grandjean, V., Gounon, P., Cuzin, F. and Rassoulzadegan, M. (2008). RNA induction and inheritance of epigenetic cardiac hypertrophy in the mouse. *Dev. Cell* **14**, 962-969.

Wolf, C. M., Moskowitz, I. P., Arno, S., Branco, D. M., Semsarian, C., Bernstein, S. A., Peterson, M., Maida, M., Morley, G. E., Fishman, G. et al. (2005). Somatic events modify hypertrophic cardiomyopathy pathology and link hypertrophy to arrhythmia. *Proc. Natl. Acad. Sci. USA* **102**, 18123-18128.

Yoshida, M., Minamisawa, S., Shimura, M., Komazaki, S., Kume, H., Zhang, M., Matsumura, K., Nishi, M., Saito, M., Saeki, Y. et al. (2005). Impaired Ca2+ store functions in skeletal and cardiac muscle cells from sarcalumenin-deficient mice. *J. Biol. Chem.* **280**, 3500-3506.